DoE Award #: DE-SC0006591

Institution: California Institute of Technology, Pasadena, CA 91125

Project Title: Towards predictive simulations of soot formation: from surrogate to turbulence

Name of PI: Guillaume Blanquart

Report Date: 3-28-17

Research period: July 2011 – July 2016

1. Objectives

The combustion of transportation fuels (e.g. kerosene, gasoline, diesel) leads to the formation of several kinds of pollutants, among which are soot particles. These particles, also formed during coal combustion and in fires, are the source of several health problems and environmental issues. Unfortunately, our current understanding of the chemical and physical phenomena leading to the formation of soot particles remains incomplete, and as a result, the predictive capability of our numerical tools is lacking.

The objective of the work was to reduce the gap in the present understanding and modeling of soot formation both in laminar and turbulent flames. The effort spanned several length scales from the molecular level to large scale turbulent transport. More precisely, the objectives were three-fold:

- develop a *single combined chemical and soot model* validated for all relevant components usually found in real fuel surrogates;
- develop a framework able to *explain the complete evolution of soot particles* from cluster of PAHs to oxidation of large fractal aggregates;
- *understand and model the interplay* between unsteady chemistry, differential diffusion, and turbulent transport.

The following sections detail the scientific accomplishments made towards these three objectives.

2. Chemical kinetics – From surrogates to PAH formation

Transportation fuels are composed of a multitude of species with very different chemical structures. In practice, these fuels are represented by surrogates consisting of a few selected species, and kinetic models are developed to describe their combustion. An accurate chemical model for soot formation requires two elements: 1) a model describing the decomposition/oxidation of the fuel components and 2) a model describing the formation/build-up of large PAH. The following sections detail improvements made in these models and the extensive validation of the models.

➔ Corrected Thermodynamic Properties

The first and most fundamental component of any chemical model is the list of thermodynamic properties, namely heat capacity $C_p(T)$, heat of formation $\Delta_f H^0$, and reference entropy S^0_{ref}. It is important to realize that these quantities control a lot more than just heat release. For any chemical reactions, the

ratio of the forward and backward rate constants is nothing more than the equilibrium constant which is purely a function of the thermodynamic properties. As such, these properties control the relative balance of each chemical reactions. Before the start of this research effort, the PI had evaluated all properties of PAH molecules (up to coronene): single point energies were computed with the G3(MP2)//B3 hybrid method combined with group corrections, and torsion potentials (for hindered rotors) were evaluated at the MP2//cc-pVDZ level. This led to an unprecedented database of consistent properties for PAH species. This database has been re-evaluated by the PI.

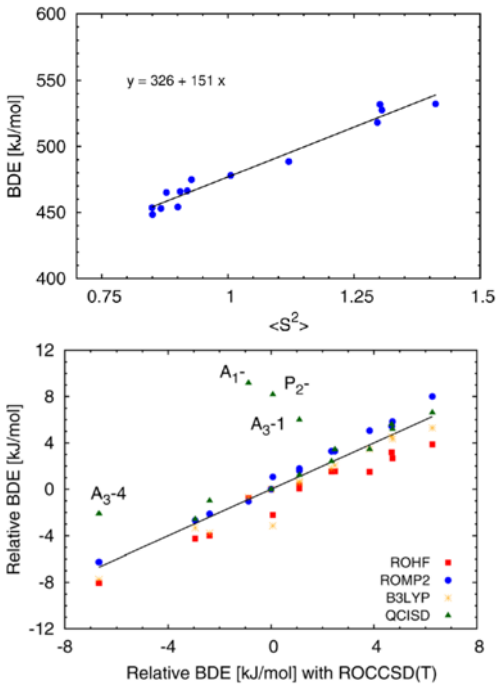

Figure 1. Errors due to spin contamination (top for UMP2) can be quite significant and can lead to incorrect bond dissociation energies (BDE) even with high order methods as QCISD(T) (bottom) **(1)**.

In computing these properties, particular care should be exercised in the selection of ab-initio methods as spin-unrestricted methods (even QCISD(T)) are subject to spin contamination errors for large PAH radicals (**Figure 1**). While not a surprising result in itself, the magnitude of these errors was found to be unexpectedly large. In fact, they were as large as deviations due to changes in the molecular structure of the PAH radicals (i.e. isomers). A combination of spin-restricted methods was used to propose new corrected thermodynamic properties for PAH radicals.

This work has been published in the International Journal of Quantum Chemistry (1).

➔ **Kinetic Mechanism – Fuel Oxidation**

The second and main component of any chemical model is the kinetic reaction scheme. In this research effort, the PI has made various contributions with

- a complete revision of C_1-C_4 chemistry,
- improved kinetics of alkane fuels, and
- updated kinetics of substituted aromatic species.

The performance of this detailed chemical model, referred to as CaltechMech, (currently composed of 173 species and 1895 reactions) has been the subject of a validation in an unprecedented number of conditions, including flow reactors, shock tubes, laminar premixed flames, and laminar diffusion flames (**Figure 2**). A wide range of single component fuels have been considered from small hydrocarbons (from methane to butadiene), aromatic fuels (from benzene to m-xylene to methyl-naphthalene), large hydrocarbon fuels (from *n*-hexane to *n*-dodecane to iso-octane), and finally small oxygenated fuels (acetaldehyde, acetone, etc).

The chemical model is available for download at http://theforce.caltech.edu/CaltechMech.

				Species profiles			
		Ignition delay-times	Flame speeds	Shocktubes	Plug flow reactors	Premixed flames	Diffusion flames
Small hydrocarbons							
Hydrogen	H2	report	report				
Methane	CH4	report	report	report pyrolysis oxidation			
Acetylene	C2H2	report	report	report pyrolysis			report
Ethylene	C2H4	report	report	report pyrolysis oxidation		report report	
Ethane	C2H6	report	report	report pyrolysis oxidation			
Allene/Propyne	C3H4	A-C3H4 P-C3H4	report				
Propene	C3H6	report	report	pyrolysis			
Propane	C3H8	report	report	report			
Diacetylene	C4H2	report		pyrolysis oxidation			
Butadiene/Butyne	C4H6	report	report	report 13-butadiene 12-butadiene 2-butyne			
Cyclopentadiene	C5H6	report	report		report		
Oxygenated species							
Formaldehyde	CH2O			report			
Methanol	CH3OH	report	report	report			
Acetaldehyde	CH3CHO			report			
Acetone	CH3COCH3		report				
Aromatic species							
Benzene	C6H6		report				
Toluene	C7H8	report	report		report		
Styrene	C8H8				report		
Ethylbenzene	C8H10	report	report		report		
Xylene	C8H10	report	report				
Methylnaphthalene	C11H10	report	report				
Large alkanes							
n-Hexane	C6H14		report				
n-Heptane	C7H16	report	1 atm high P	report pyrolysis		report report report	report
iso-Octane	C8H18		1 atm high P			report	
n-Dodecane	C12H26	report	report	report pyrolysis			

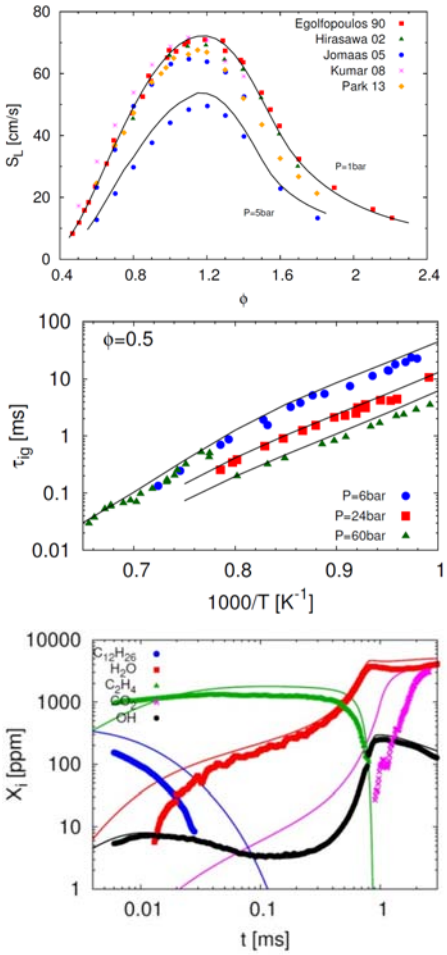

Figure 2. Left: fuels and configurations used for the validation of the CaltechMech v2.3 model. Right: examples of known performances: ethylene flame speed, propane ignition delay times, species profiles in *n*-dodecane shock tube (top to bottom).

➔ Surrogate Formulation

JP-8 was selected as a representative transportation fuel in this research and its combustion was investigated in laminar and turbulent flames. The combustion of JP-8 fuel was represented with a surrogate composed of 77% of *n*-dodecane and 23% of m-xylene (by volume). Using the chemical model presented previously (i.e. CaltechMech), ignition delay times, laminar flame speeds, and a laminar premixed flame have been considered as test cases for the validation of the surrogate formulation (**Figure 3**).

The overall agreement between the laminar flame speeds predictions and the measurements was found to be very good for most equivalence ratios. Given the fact that the surrogate formulation is a weighted average of pure *n*-dodecane and pure m-xylene, the flame speeds were observed to fall between the values for the pure fuels. In laminar rich premixed flame of kerosene/air, the main products of combustion were predicted accurately by the chemical model and the yields of soot precursors were also well reproduced.

This surrogate formulation was used in LES of turbulent flames (see below).

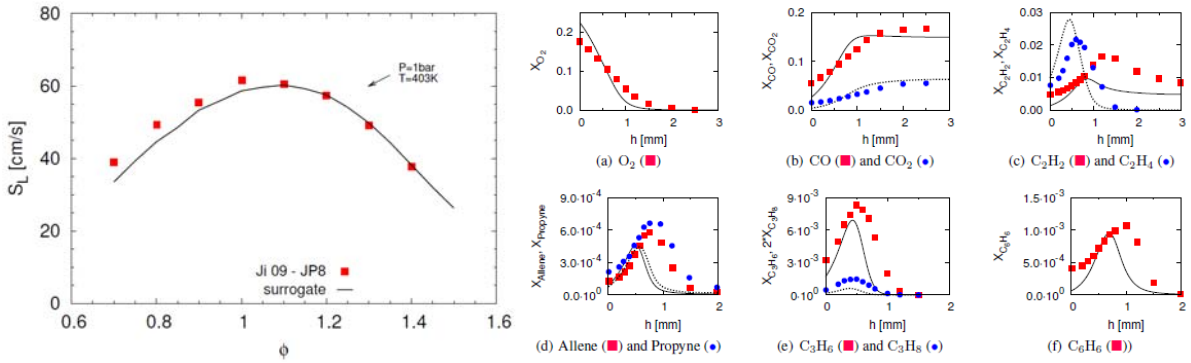

Figure 3. Laminar burning velocities for JP-8 in air (left) and species profiles in a laminar premixed flame (right).

➔ Two-Dimensional Effects in Laminar Premixed Flames

Burner-stabilized, axisymmetric, laminar premixed flames have been used for a long time for the development of PAH and soot models. Numerical simulations of these flames always rely on the assumption of one-dimensionality. However, the presumed one-dimensionality has not been justified in general, and may not be valid under all circumstances. That is why, we investigated two-dimensional flow effects in various key ethylene/air laminar premixed flames, which had been selected as validation targets for the International Sooting Flame (ISF) workshop. These flames covered all typical experimental arrangements, namely stabilizing plate, steel plate with centered hole, and enclosed chamber.

To assess the assumption of one-dimensionality, detailed numerical simulations with finite-rate chemistry were performed with the exact experimental set-ups. It was shown that flow entrainment and acceleration are significant for all four flames (Figure 4). Further, it was found that the flame centerlines cannot be approximated as one-dimensional, since the mass flow rates vary substantially along the centerlines. As a consequence, non-negligible differences were found between the soot profiles predicted in two-dimensional simulations and in simulations where one-dimensionality was assumed. Using data extracted from the two-dimensional simulations, a modified one-dimensional model was derived on the flame centerline to include two-dimensional effects.

This work has been published in Combustion and Flame (2).

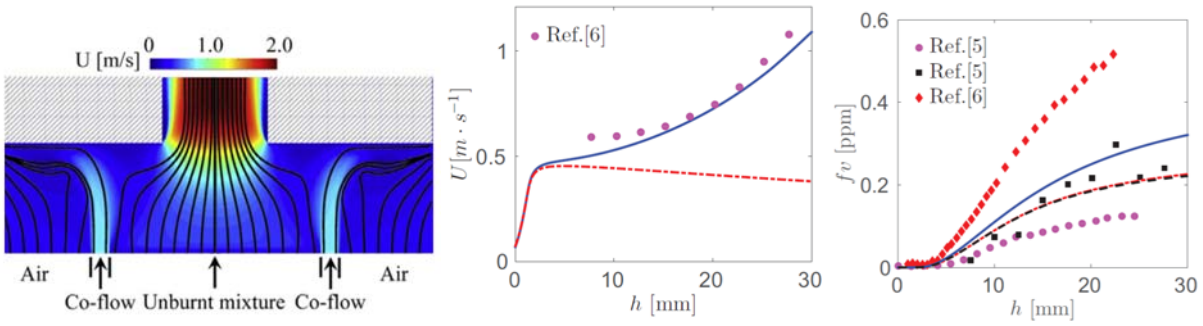

Figure 4. Results of a two-dimensional numerical simulation of the ISF target flames: contour of velocity (left), centerline velocity (center) from 2D (solid) and 1D calculations (dashed), and soot volume fraction (right).

➔ **Predicting Sooting Tendencies**

Axisymmetric coflow diffusion flames have been used extensively to measure experimentally the sooting tendencies of various fuels/compounds. Unfortunately, these sooting indices had not yet been used to test the accuracy of chemical models.

The intent of our work was to predict experimentally-observed sooting tendencies of different fuels from a detailed chemical mechanism at low computational cost. Towards that goal, direct numerical simulations using finite-rate chemistry were conducted on a methane-air confined axisymmetric co-flow diffusion flame to provide reference data. Sooting tendencies were estimated from the increment of polycyclic aromatic hydrocarbon (PAH) dimer production rate along the centerline when the flame is doped.

Calculations using the conventional steady state diffusion flamelet model were performed and this model was shown to be inadequate in reproducing the correct species profiles on the centerline of the flame. The main reason for this failure is the neglect of multidimensional convection and diffusion effects. In an effort to overcome these deficiencies, we proposed a new numerical framework based on *modified* flamelet equations. The flamelet equations were re-derived for species mass fractions along the centerline of the co-flow diffusion flame considered. These equations take into account the effects of multidimensional diffusion and convection of species in mixture fraction space due to non-unity Lewis numbers. The modified flamelet equations take as input the temperature, convective velocity, and scalar dissipation rate profiles calculated from the direct simulation of the diffusion flame.

The numerical sooting tendencies for both non-aromatic and aromatic test species were then calculated using the PAH dimer production rate generated from the flamelet solutions doped by the test species. These first numerically-computed sooting tendencies were derived from a detailed chemical kinetic mechanism and were in good agreement when compared to experimental values (**Figure 5**). This provides an additional level of validation of the kinetic mechanism for PAH formation.

This work has been published in Combustion and Flame (3) with a follow up analysis in (4).

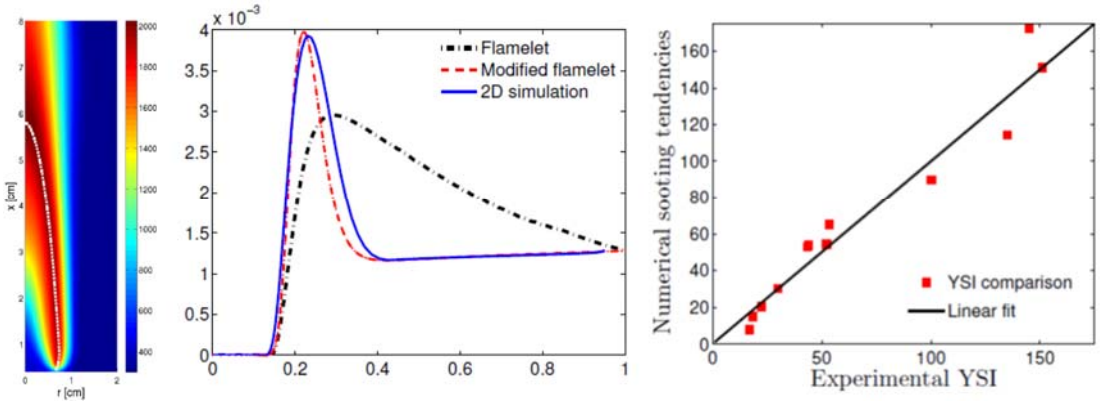

Figure 5. Temperature for the coflow diffusion flame (left). Comparison of dopant mass fraction profiles for the conventional and modified flamelet models (center). Comparison of experimentally-measured YSI and numerically computed YSI (right).

3. Soot Evolution – From particle Inception to Oxidation

As a co-leader and active participant of the International Sooting Flames (ISF) workshops, we simulated a large number flames (from 1D laminar to 3D turbulent flames) in an attempt to evaluate the predictive nature of the recent developments we made in terms of chemistry/PAH/soot modeling.

➔ Laminar Premixed Flames

One-dimensional, burner-stabilized, laminar premixed flames have been used for a long time for the development of PAH and soot models. For the last two ISF workshops, the PI was in charge of selecting the target flames, collecting the results, and summarizing findings for the laminar premixed flames section. A total of 25 flames covering 6 different burner configurations were selected. To help the community simulate these flames and to provide a common basis for comparison between models, we simulated all flames ahead of the workshops and provided an experimentally-consistent, numerically-simulated temperature profile for each flame. These profiles were used by all research groups in their simulations. Our results indicated that 1) large deviations are often observed between experimentally-measured and numerically-simulated temperature profiles, 2) soot volume fractions are always predicted within a factor of two or three if the "correct" temperature profile is used, and 3) soot particle diameters were only predicted with enough accuracy if aggregates and non-purely spherical particles were considered.

➔ Laminar Coflow Diffusion Flames

Coflow diffusion flames present an intermediate configuration in terms of complexity and relevance between laminar premixed flames and turbulent diffusion flames. We selected three flames among the ISF target flames and simulated them with our recently improved chemical/soot models. Once again, some deviations we observed between experimentally-observed and numerically simulated temperature profiles were observed (see Figure 6). Consistent with the results of the premixed flames, soot volume fraction was predicted with a factor of two or three on the "wings" of the coflow diffusion flames. Yet, it was always under-predicted along the centerline, showing limitation in our nucleation model and highlighting the need for an improved PAH to soot inception model.

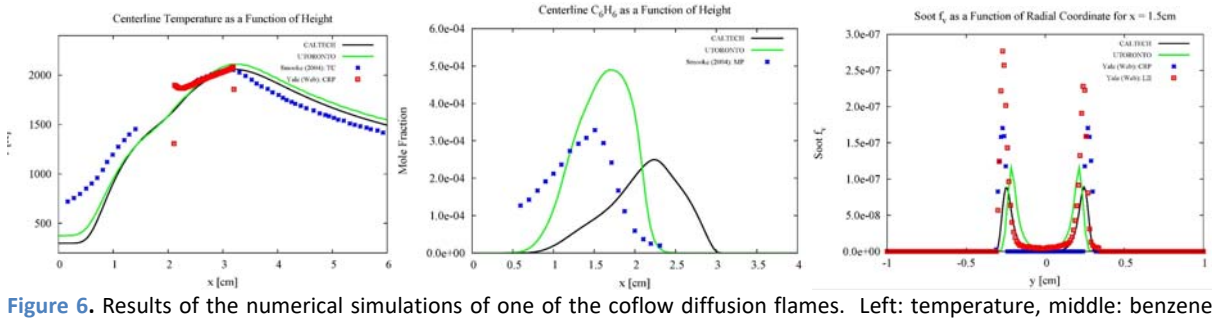

Figure 6. Results of the numerical simulations of one of the coflow diffusion flames. Left: temperature, middle: benzene mole-fractions, and right: soot volume fraction.

➔ Soot Nucleation from Excimers

Following the results obtained in the above laminar premixed and coflow diffusion flames, we identified soot nucleation as one of the major sources of error in our predictions (a common observation at ISF).

Most models base soot nucleation upon the dimerization of gas phase PAHs that arises through collisions between these gaseous molecules. These models contain three major flaws and ultimately violate the second law of thermodynamics. First, soot particles are formed at all temperatures, including room temperature, a phenomenon that is not observed experimentally. Second, these models predict that collisions between aromatic molecules of any size, including benzene, will form a soot particle. Third, the dimers produced by these collisions are predicted to be infinitely stable.

In an attempt to correct for the first two issues, we hypothesized that only collisions that included at least one excited state PAH, which would not be found at low temperatures, could form a stable dimer. Preliminary calculations of the energy difference between excited and ground states were performed at the B3LYP level with the Dunnings Correlation Consistent basis sets. The results suggest that, while the excitation energy negatively correlated with molecular weight, it was strongly dependent upon the structure of the given PAH (Figure 4). PAHs that more closely resembled the *n*-acenes in structure had lower excitation barriers than other PAHs of similar mass. Using the calculated excitation energies, we evaluated the population of excited states at a given temperature assuming a Boltzmann equilibrium distribution. We found that only higher mass PAHs, particularly anthracene and tetracene, form a sufficiently large population of excited molecules at common sooting flame temperatures.

To tackle the third issue presented by current models, we used benzene and naphthalene as test cases to determine the stability of any excimers formed from a successful collision. Preliminary calculations were carried out using the MP2/cc-PVDZ level of theory. We compared the energy of two molecules, one in its ground and one in its excited state, an ”infinite distance” apart to two in close proximity (3-4 angstroms) and found that, for benzene, dimerization provides significant stabilization to the two molecules (30 kJ/mol) (see **Figure 7**).

While preliminary, the present results suggest that a collision-based model involving one ground state and one excited state PAH might play a role in soot nucleation. Obviously, further work is necessary.

These results were shown at the 8th US National Meeting of the Combustion Institute (5).

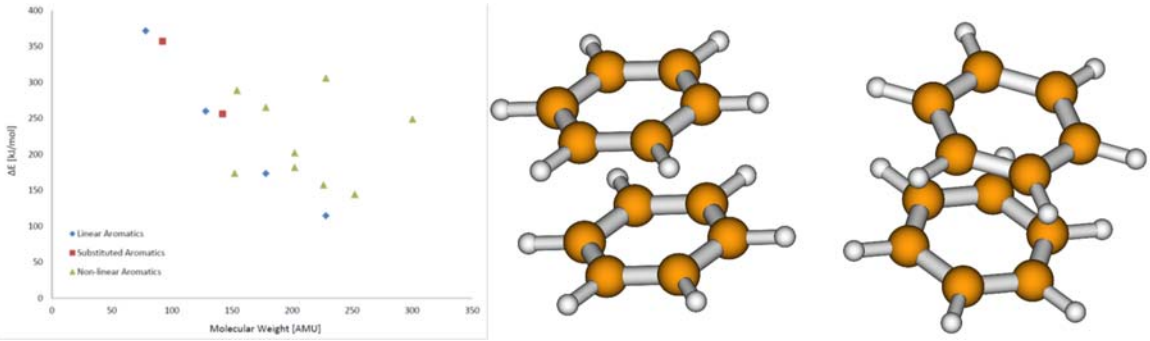

Figure 7. Energy difference between ground state and first excited state for a series of PAH molecules (left). Two different configurations of a benzene excimer (parallel – center; rotated – right).

4. Soot-Turbulence Interactions

The investigation of soot-turbulence interactions started with a theoretical investigation followed by Large Eddy Simulations of experimentally-measured sooting turbulent jet diffusion flames.

➔ PAH Relaxation Model for Soot Formation in Turbulent Flames

The chemical response of different species to turbulent effects was investigated in the context of one-dimensional laminar non-premixed flamelets. Turbulent effects were modeled as abrupt changes in the scalar dissipation rate. For consistency with the turbulent flames to be simulated (next section), an ethylene/air configuration was selected.

From the time-evolution of the species mass fractions, it was found that transient effects are not substantial for radicals such as OH and H, and species such as CO,CO_2 and C_2H_2, consistent with their small characteristic chemical time scales. The steady state flamelet assumption for these species is well justified and their mass fractions can be pre-tabulated using the steady state flamelet solutions legibly. On the other hand, aromatic species are characterized by relatively slow chemistry, and substantial transient effects were observed for these species. The evolution of their mass fractions and chemical source terms was further studied through a reaction flux analysis. For PAH, the chemical production terms were found to be linearly proportional to the mass fraction of smaller aromatic species, and the chemical consumption terms were found to be linearly proportional to their own mass fractions (see **Figure 8**). Based on the unsteady flamelet results, the validity of various existing flamelet-based pre-tabulation methods was examined, and a new linear relaxation model was proposed for PAH.

This work has been published in Combustion and Flame (6).

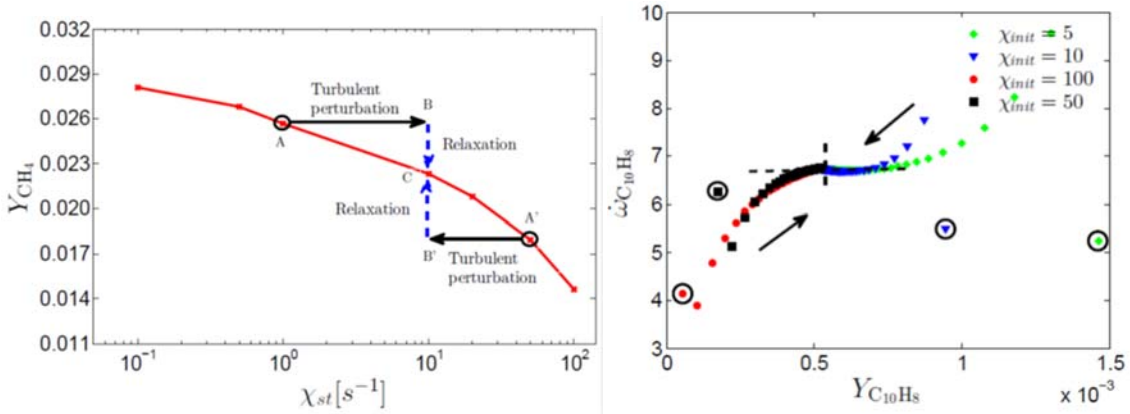

Figure 8. Overview of the chemistry relaxation model under turbulent fluctuations (left). Dependence of chemical source term on the species mass fraction for naphthalene for various initial scalar dissipation rates (right).

➔ Large Eddy Simulations

Large Eddy Simulations (LES) have been performed on an ethylene/air piloted turbulent non-premixed sooting jet flame to quantify the importance of aromatic chemistry-turbulence interactions (see previous section). The simulation framework relies on four major components: a gas-phase chemistry model, a turbulence closure model, a PAH relaxation model, and finally a soot model.

First, the combustion processes were described using the flamelet/progress variable (FPV) approach, extended to include radiative heat losses in the limit of optically thin medium. Second, all sub-filter fluxes were closed using a dynamic Smagorinsky model with Lagrangian averaging techniques. The filtered thermochemical quantities were obtained from the equation of state by convolution with a joint sub-filter

PDF. Third, soot formation depends critically on the concentrations of its precursors, namely aromatic species, which exhibit substantial transient effects due to turbulent unsteadiness. To account for these effects, transport equations were solved for their mass fractions. The chemical source terms for these transported aromatic species were closed using the previously-discussed relaxation model. Finally, the geometry of fractal soot aggregates was described using a bi-variate description based on its total volume V and total surface area S. The evolution of soot particles was described, from a statistical point of view, by solving the transport equations for several key moments, and their source terms were closed using the Direct Quadrature Method of Moments (DQMOM).

Sooting Ethylene Flame

The models were integrated into LES of a non-premixed ethylene/air piloted turbulent jet flame, experimentally investigated at Sandia National Laboratories by Dr. Shaddix. This flame was selected over other experimentally studied turbulent non-premixed flames, for its relatively large soot yield, high Reynolds number, and well-defined boundary conditions.

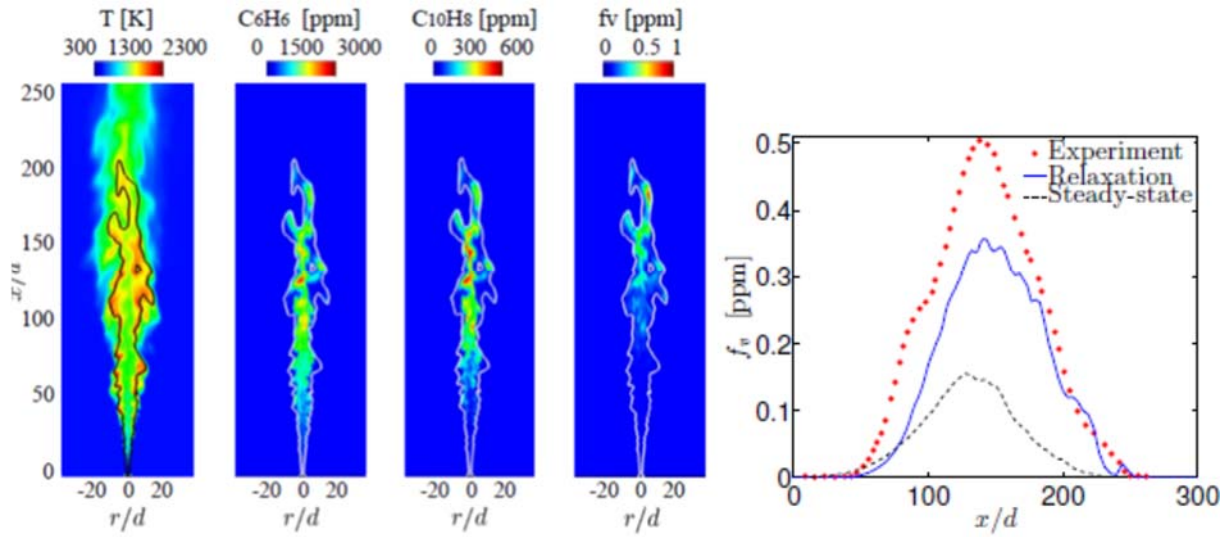

Figure 9. Instantaneous fields of temperature, benzene mass fraction, naphthalene mass fraction, and soot volume fraction (from left to right). Mean soot volume fraction on the flame centerline (right).

As expected, the yield of aromatic species and soot was predominant in fuel rich regions, with benzene forming at x/d=15 and naphthalene at x/d=30 (**Figure 9**). Soot formation occurred at locations even more downstream at x/d=50. These lags in formation locations reflect the combined effects of the sequential formation of aromatic species and soot, and the large time scales governing their formation.

Figure 9 also shows the time-averaged soot volume fractions on the flame center-line from two LES and from laser-induced incandescence measurements. Comparisons with experimental results indicate that the LES using the previously-derived PAH relaxation model predicted the mean soot distribution reasonably accurately. On the other hand, the steady-state LES (without the PAH relaxation model) predicted a lower soot yield and a slightly shifted soot profile towards the burner exit.

Turbulence-chemistry interaction impacts not only mean quantities, but also the fluctuations in soot (**Figure 10**). Both the mean value and the magnitude of fluctuations (width of the PDF) are well captured by

the relaxation LES; although occurrence of low soot volume fractions (fv < 0.2 ppm) is slightly over-predicted. In contrast, the steady-state LES predicts a lower mean, as aforementioned, and significantly smaller fluctuations (narrower PDF).

This work has been published in the Proceedings of the Combustion Institute (7).

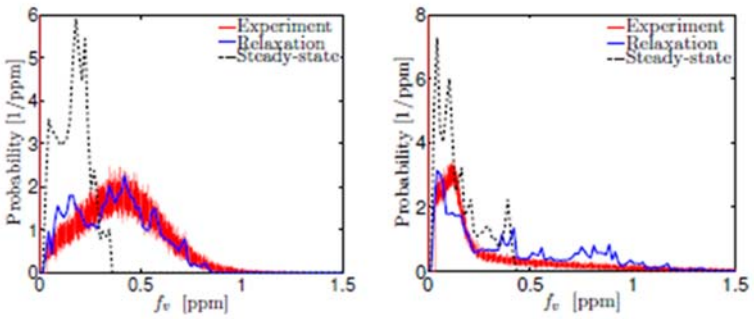

Figure 10. PDFs of soot volume fraction at two locations on the flame centerline.

Sooting Kerosene Flame

We performed one of the first LES of a turbulent sooting flame burning a kerosene surrogate (77% *n*-dodecane/ 23% *m*-xylene). These preliminary simulations were intended to reproduce a piloted turbulent diffusion flame experiment performed at Sandia Nat Labs by Shaddix et al. (**Figure 11**) and were performed using the same modeling approaches as described previously.

These simulations highlighted computational challenges associated with large density ratios in low Mach flow solvers. Improving the numerical time integration scheme should be the subject of future work.

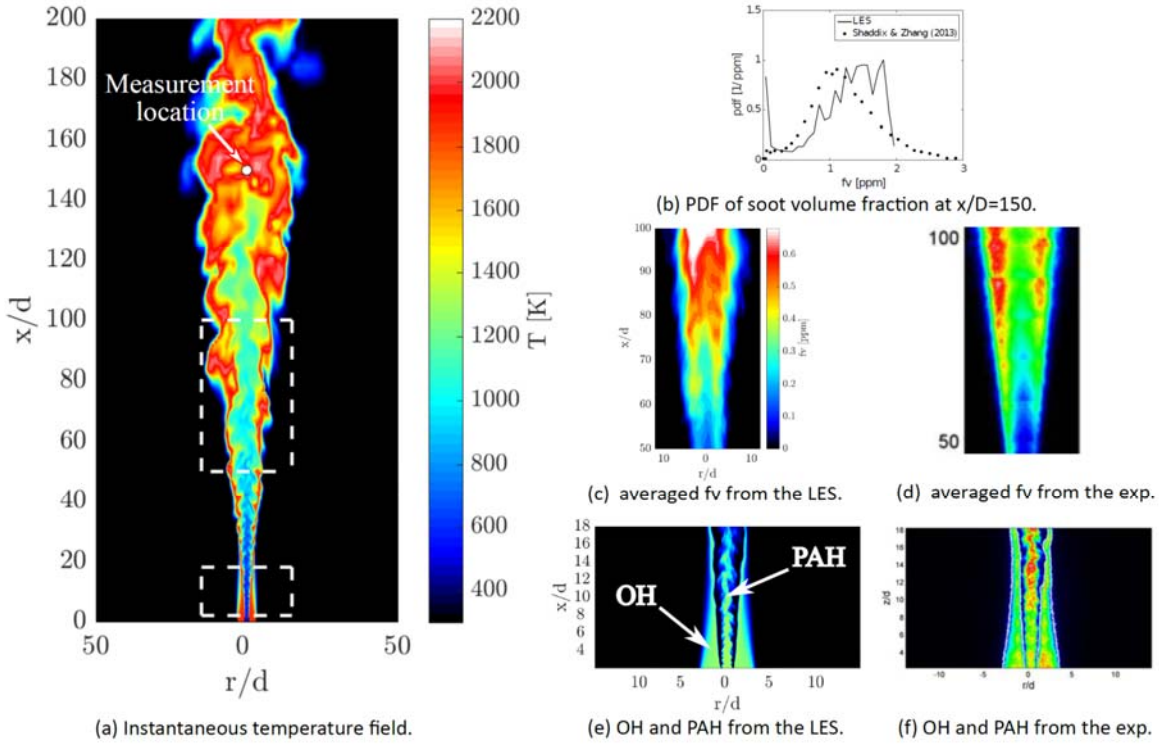

Figure 11. Preliminary results of an LES of a turbulent, sooting, diffusion flame of a kerosene surrogate.

➔ **Turbulent/Effective Lewis Numbers**

In many combustion modeling approaches (such as in tabulated chemistry), the species Lewis numbers (ratio of heat diffusion to mass diffusion) are used as input parameters. While it is well-accepted that these Lewis numbers tend toward unity under intense turbulence, it is unclear what their values are for "less turbulent" conditions and for heavy hydrocarbon species as found in kerosene fuels and for soot precursors (PAH species). Using incorrect Lewis numbers could lead to factors of two to three variations in soot nucleation rates.

The goal of this preliminary work was to develop simple, physics-based correlation functions to relate these turbulent Lewis numbers in terms of the local Reynolds number. We proposed a methodology to extract these turbulent Lewis numbers from experimental measurements of species mass fractions conditioned on mixture fraction (**Figure 12**). This approach has been applied so far to the series of Sandia B through E flames of the Turbulent Non-premixed Flames (TNF) workshop.

This work has been submitted for publication to Combustion and Flame (8).

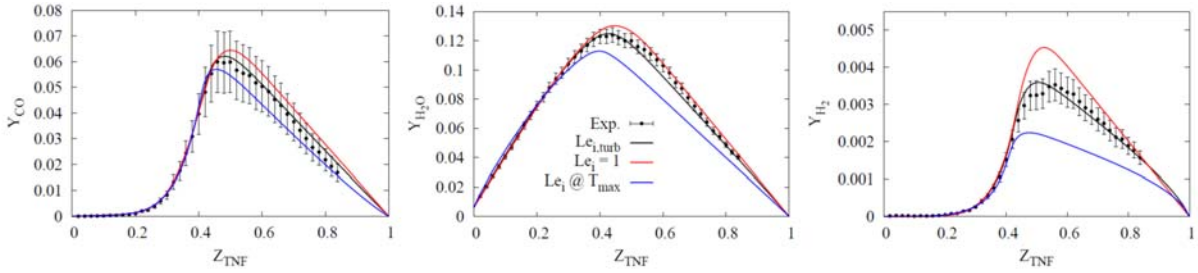

(a) CO mass fraction. (b) H_2O mass fraction. (c) H_2 mass fraction.

Figure 12. Comparison of measured species conditional mean mass fractions for Sandia flame C at x/D=30, against the flamelet solutions corresponding to turbulent Lewis numbers (black line), unity Lewis numbers (red line), and laminar Lewis numbers (blue line).

➔ **Accelerating Numerical Simulations with Detailed Chemistry**

The previous theoretical and LES studies have highlighted even more the need for Direct Numerical Simulations (DNS) with detailed chemistry to probe the intricate coupling between turbulence, chemistry, and soot formation. However, these simulations are computationally very expensive. In an attempt to reduced computational cost while maintaining numerical accuracy, we have undertaken multiple preliminary studies, leading to revisions of the numerical methods used.

Stiff Chemistry Time Integration

First, we proposed a semi-implicit preconditioned iterative method for the time-integration of the stiff chemistry in simulations of unsteady reacting flows, such as turbulent flames, using detailed chemical kinetic mechanisms. Emphasis was placed on the simultaneous treatment of convection, diffusion, and

chemistry, without using operator splitting techniques. The preconditioner corresponds to an approximation of the diagonal of the chemical Jacobian. Upon convergence of the sub-iterations, the fully-implicit, second-order time-accurate, Crank–Nicolson formulation is recovered.

Performance of the proposed method was tested theoretically and numerically on one-dimensional laminar and three-dimensional high Karlovitz turbulent premixed *n*-heptane/air flames. The species lifetimes contained in the diagonal preconditioner were found to capture all critical small chemical timescales (**Figure 13 - left**), such that the largest stable time step size for the simulation of the turbulent flame with the proposed method is limited by the convective CFL, rather than chemistry. The theoretical and numerical stability limits are in good agreement and are independent of the number of sub-iterations. The results indicated that the overall procedure is second-order accurate in time, free of lagging errors, and the cost per iteration is similar to that of an explicit time integration. The theoretical analysis was extended to a wide range of flames (premixed and non-premixed), unburnt conditions, fuels, and chemical mechanisms. In all cases, the proposed method was found (theoretically) to be stable and to provide good convergence rate for the sub-iterations up to a time step size larger than 1 µs. This makes the proposed method ideal for the simulation of turbulent flames.

This work has been published in the Journal of Computational Physics (9).

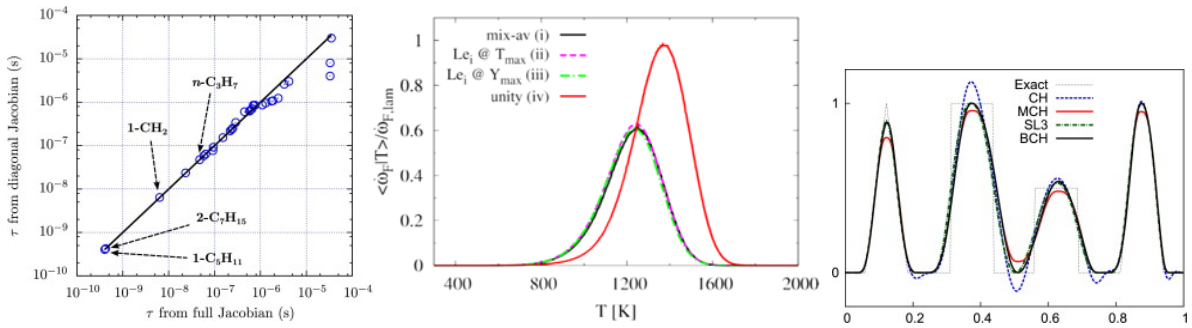

Figure 13. Comparison of chemical timescales from full Jacobian and the preconditioner (left); comparison of conditional mean fuel source terms with different diffusion models (center); comparison of scalar profiles obtained with different scalar transport schemes (right).

Species Diffusion Model

Accurate computation of molecular diffusion coefficients in chemically reacting flows can be an expensive procedure, and the use of constant non-unity Lewis numbers has been adopted often as a cheaper alternative. We explored the validity and the limitations of such approach in the description of molecular mixing in laminar and turbulent flames.

To carry out this analysis, three test cases have been selected, including a lean, highly unstable, premixed hydrogen/air flame, a lean turbulent premixed *n*-heptane/air flame, and a laminar ethylene/air coflow diffusion flame. For the hydrogen flame, both a laminar and a turbulent configuration have been considered. The three flames are characterized by Lewis numbers which are less than unity, greater than unity, and close to unity, respectively. For each flame, mixture-averaged transport simulations were carried out and used as reference data. The analysis suggested that, for numerous combustion configurations, the

constant non-unity Lewis number approximation leads to small errors when the set of Lewis numbers is chosen properly (**Figure 13 - center**). For the selected test cases and our numerical framework, the reduction of computational cost is found to be minimal.

This work has been published in Combustion, Theory and Modelling (10).

Transport of Low Diffusivity Scalar

Third, we proposed an improved bounded semi-Lagrangian scheme for soot transport based on cubic Hermite polynomial reconstruction. Boundedness of the scalar being transported (here soot concentration) is ensured by applying derivative limiting techniques. Single sub-cell extrema are allowed to exist as they are often physical, and help minimize numerical dissipation. The proposed bounding algorithm, although a seemingly subtle difference from strict monotonicity enforcement, was shown to result in significant performance gain in laminar cases, and in three-dimensional turbulent mixing layers.

The scheme satisfies several important properties, including boundedness, low numerical diffusion, and high accuracy (**Figure 13 - right**). Performance gain in the turbulent case was assessed by comparing scalar energy and dissipation spectra produced by several bounded and unbounded schemes. The results indicated that the proposed scheme is capable of furnishing extremely accurate results, with less severe resolution requirements than all the other bounded schemes tested. Additional simulations in homogeneous isotropic turbulence show good agreement with spectral scheme results available in the literature. Detailed analytical examination of gain and phase error characteristics of the original cubic Hermite polynomial was also performed, and pointed to dissipation and dispersion characteristics comparable to, or better than, those of a fifth order upwind Eulerian scheme.

This work has been published in the Journal of Computational Physics (11).

Filtering in the viscous-convective subrange

Despite all these previous numerical improvements, DNS of soot formation remain particularly expensive because of the requirement of resolving all physical length scales down to Batchelor's scale. In an attempt of reducing the overall computational cost, we have investigated the possibility of resolving only the velocity scales (down to Kolmogorov's length scale) and filtering out all smaller scales.

The major challenge in performing the proposed simulations is obtaining a closed form for the sub-filter scalar flux (SFF) term. We analyzed the assumptions and consequences behind filtering in the viscous-convective subrange using DNS data. Several key observations were made. First, the magnitude of the SFF term decreases exponentially with cut-off wavenumber. Second, this magnitude is independent of the Reynolds number. These two observations justify the use of DNS even at low Reynolds numbers to analyze the form of the SFF term.

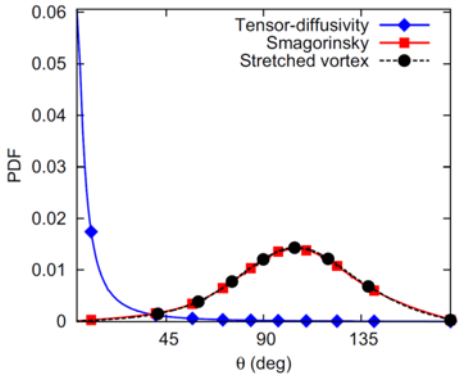

Figure 14. PDFs of the angle between the true SFF vector and the model predictions.

In a second study, we analyzed the alignment of the SFF vector in the eigenframe of the strain-rate tensor. Combining results on the orientation of vorticity and scalar gradient vectors in this frame, we proved that the tensor diffusivity model provides a near analytical closed form of the SFF vector (**Figure 14**). This general result, valid for Gaussian and Box filters, was obtained using a simple Taylor expansion. More importantly, the above expression is exact for a locally-linear velocity field. Hence, this model is compatible with the assumption of Batchelor's theory, namely material elements experience effectively linear straining.

While only preliminary, this work shows great opportunies for reducing the computational cost of numerical simulations of soot formation. This work has been published in Physics of Fluids (12) and in Physical review E (13).

5. Contributing Students/Postdocs

Several students and postdoctoral scholars have contributed to this research effort:

- Andrew Barlett – Undergraduate Student – 10 weeks – 100%
- Nicholas Burali – Graduate Student – 6 months – 100%
- Phares Carroll – Graduate Student – 1 month – 100%
- Emmet Cleary – Undergraduate Student – 10 weeks – 100%
- Jeff Rah – Graduate Student – 6 months – 100%
- Bruno Savard – Graduate Student – 1 month – 100%
- Jason Schlup – Graduate Student – 11 months – 100%
- Sid Verma – Graduate Student – 32 months – 100%
- Pauline Vervisch-Kljakic – Postdoctoral Scholar – 3 months – 100%
- Yuan Xuan – Graduate Student – 35.5 months – 100%

6. Bibliography

1. *Effects of Spin Contamination on Estimating Bond Dissociation Energies of Polycyclic Aromatic Hydrocarbons.* **Blanquart, G.** 2015, International Journal of Quantum Chemistry, Vol. 115, pp. 796–801.

2. *Two-dimensional flow effects on soot formation in laminar premixed flames.* **Xuan, Y. and Blanquart, G.** 2016, Combustion and Flame, Vol. 166, pp. 113–124.

3. *Numerical Modeling of Sooting Tendencies in a Laminar Co-flow Diffusion Flame.* **Xuan, Y. and Blanquart, G.** 2013, Combustion and Flame, Vol. 160, pp. 1657-1666.

4. *Modeling curvature effects in diffusion flames using a laminar flamelet model.* **Xuan, Y., Blanquart, G. and Mueller, M.E.** 2014, Combustion and Flame, Vol. 161, pp. 1294-1309.

5. *Investigation into the Mechanism of Soot Deposition from Gaseous Polycyclic Aromatic Hydrocarbons.* **Bartlett, A. and Blanquart, G.** Salt Lake City, UT : s.n., 2013. 8th US Combust. Meet.

6. *A flamelet-based a priori analysis on the chemistry tabulation of polycyclic aromatic hydrocarbons in non-premixed flames.* **Xuan, Y. and Blanquart, G.** 2014, Combustion and Flame, Vol. 161, pp. 1516–1525.

7. *Effects of aromatic chemistry-turbulence interactions on soot formation in a turbulent non-premixed flames.* **Xuan, Y. and Blanquart, G.** 2015, Proceedings of the Combustion Institute, Vol. 35, pp. 1911-1919.

8. *Effective Lewis numbers in turbulent non-premixed flames.* **Burali, N. and Blanquart, G.** submitted, Combustion and Flame.

9. *A computationally-efficient, semi-implicit, iterative method for the time-integration of reacting flows with stiff chemistry.* **Savard, B., et al.** 2015, Journal of Computational Physics, Vol. 295, pp. 740–769.

10. *Assessment of the constant non-unity Lewis number assumption in chemically-reacting flows.* **Burali, N., et al.** 2016, Combustion Theory Modelling, Vol. 20, pp. 632-657.

11. *An improved bounded semi-Lagrangian scheme for the turbulent transport of passive scalars.* **Verma, S., Xuan, Y. and Blanquart, G.** 2014, Journal of Computational Physics, Vol. 272, pp. 1-22.

12. *On Filtering in the Viscous-Convective Sub-range for Turbulent Mixing of High Schmidt Number Passive Scalars.* **Verma, S. and Blanquart, G.** 2013, Phys. Fluids, Vol. 25, p. 055104.

13. *Subfilter scalar-flux vector orientation in homogeneous isotropic turbulence.* **Verma, S. and Blanquart, G.** 2014, Physical Review E, Vol. 89, p. 063015.